# Inter-Annual Variability of Salinity in the Upper Layer of South Eastern Arabian Sea and Its Acoustic Relevance

Anjali K.S.\*, P.A. Maheswaran<sup>\$,\*</sup>, K. Satheesh Kumar<sup>\$</sup> and Dominic Ricky Fernandez<sup>\$</sup>

\*Cochin University of Science and Technology, Kochi - 682 022, India \*DRDO-Naval Physical and Oceanographic Laboratory, Kochi - 682 021, India \*E-mail:: maheswaran.npol@gmail.com

#### **ABSTRACT**

This study investigates the seasonal dynamics and inter-annual variability of low-salinity Bay of Bengal Water (BBW) and Arabian Sea High Salinity Water (ASHSW) in the South Eastern Arabian Sea (SEAS). Using HadISST temperature and salinity data (2016–2020), OSCAR ocean current data, and water mass indices, we analyze the seasonal evolution and interactions of these water masses. During winter, the East India Coastal and North Equatorial Current transport low-saline waters to southern India, forming an anticyclonic eddy that recirculates BBW southwestward. By June, these waters dissipate, replaced by the expansion of ASHSW driven by summer monsoon circulation, with increasing core salinity values observed at shallower depths. Monthly salinity difference plots reveal peak BBW intrusion in November, with spreading occurring south-westward and moving northward along the coast. BBW in the SEAS exhibits strong seasonality with minimal inter-annual variability. Acoustic propagation modeling highlights the significant influence of BBW and ASHSW on sound speed profiles, with deeper sonic layer depth and strong sound speed gradients facilitating long-range ducted propagation during BBW intrusion periods.

**Keywords:** Arabian sea high salinity water mass; Bay of Bengal water mass; Southeastern Arabian sea; Circulation; Acoustic propagation

### 1. INTRODUCTION

The near-surface salinity structure show marked contrast between the Bay of Bengal and the Arabian Sea, two neighbouring basins in the northern part of the Indian Ocean. In the BoB, surface salinity remains consistently under 34 psu across all seasons due to a higher rate of precipitation compared to evaporation and the influx from major rivers<sup>1-2</sup>. Han and McCreary highlighted the importance of incorporating freshwater fluxes at the surface and through flows from adjacent seas to accurately simulate the seasonal sea surface salinity (SSS) variability in the Indian Ocean<sup>3</sup>.

Conversely, the Arabian Sea experiences higher SSS levels, generally exceeding 35 psu, due to higher evaporation rates and the lack of major river systems, except along India's west coast<sup>4-6</sup>. Numerous observational<sup>7-10</sup> and modeling studies<sup>11-13</sup> have examined the seasonal variations in upper ocean salinity in the Arabian Sea.

One distinguishing characteristics of the South Eastern Arabian Sea (SEAS) is the inflow of low-saline waters<sup>14-17</sup>, primarily originating from BoB. In winter, the presence of low-salinity Bay of Bengal Water (BBW) increases, resulting in the development of a strong halocline in the surface layer. Additionally, the summer monsoon brings heavy rainfall, leading to the formation of pronounced haline fronts near the SEAS coast. These significant haloclines can greatly impact the sound speed profile, thereby affecting acoustic propagation

Received: 03 March 2025, Revised: 14 June 2025

Accepted: 09 September 2025, Online published: 04 November 2025

characteristics in the region. Thus, a comprehensive understanding of the salinity structure, especially within the upper 200 m of the SEAS water column, is essential for accurately assessing and predicting acoustic propagation properties in this dynamic marine environment.

### 2. METHODOLOGY

### 2.1 Data Sources

This study utilizes monthly temperature and salinity datasets from the Hadley Centre Sea Ice and Sea Surface Temperature (HadISST), spanning 2016-2020, to analyze the characteristics of water masses in the Arabian Sea. The HadISST dataset provides comprehensive monthly Sea Surface Temperature (SST) and sea ice concentration globally, at 1-degree spatial resolution and extending to a depth of 5000 m (42 depth levels).

### 2.1.1 Ocean Currents Data

To study the circulation patterns in the SEAS, we used data from the OSCAR (Ocean Surface Current Analysis Real-time - distributed through NOAA and PO.DAAC), which offers ocean surface current estimates on a 1/3° spatial grid and a 5-day temporal resolution. This data set derives near-surface current velocities by applying quasi-linear, steady-state momentum equations, incorporating inputs such as sea surface height, wind vectors, and sea surface temperature. These inputs are sourced from a combination of satellite observations and in situ measurements.

### 2.1.2 Water Mass Indices

To examine the inter-annual variability of Arabian Sea High Salinity Water (ASHSW) and BBW intrusion and spreading in the SEAS, two water mass indices were introduced. These indices were based on the number of depth bins meeting specific conditions within the domain of 7° to 15°N and 68° to 78°E. For ASHSW, conditions included a density range of 1023 to 1025 kg/m³ and salinity exceeding 35.5 psu, while for BBW, conditions involved a density below 1022 kg/m³ and salinity below 35 psu.

# 2.2 Study Region

The SEAS is a region of significant interest in physical oceanography due to its complex and dynamic oceanographic and atmospheric interactions. Influenced by seasonal monsoons, freshwater influx from rivers, and exchanges with adjacent water bodies, particularly the Bay of Bengal (BoB), the SEAS exhibits unique hydrographic and thermodynamic characteristics. The interaction of riverine freshwater influx and strong wind-driven mixing and advection of water masses creates a dynamic environment with marked spatial and temporal variability in salinity structure, particularly confined to the upper 200 m.

Understanding the salinity structure in the SEAS is crucial for various applications, including marine biology, fisheries, and naval operations, as accurate salinity profiles are essential for predicting acoustic propagation, which is vital for submarine communication and navigation.

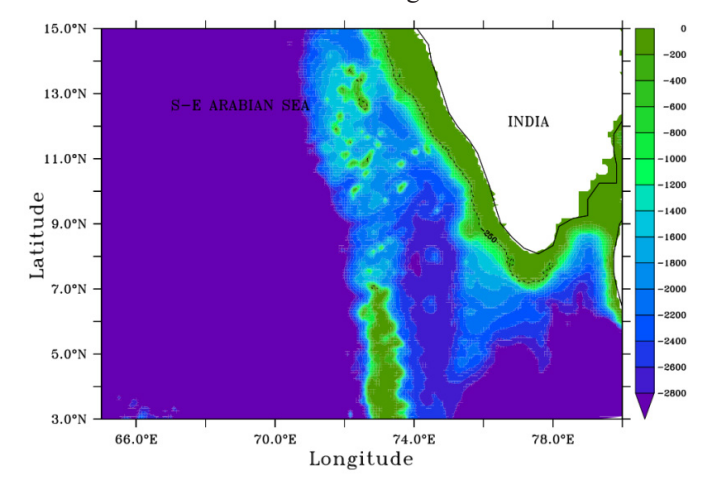


Figure 1. Geographic location and bathymetric map of the Southeastern Arabian Sea.

## 3. RESULT AND DISCUSSION

# 3.1. Surface circulation and Surface Salinity Variation in the SEAS

Sea Surface Salinity (SSS) variation associated with surface circulation in the SEAS from October 2016 to September 2017 is illustrated in Fig. 2. The contour lines of salinity exhibit a distinct meridional pattern, with lower values observed on the eastern side and higher values on the western side. For example, in October, the 34 psu contour observed in the southern Bay of Bengal region and it gradually spreads towards the SEAS with time. Salinity frontal patterns are well-marked and visible until December, as indicated by the 35 and 36 psu contours.

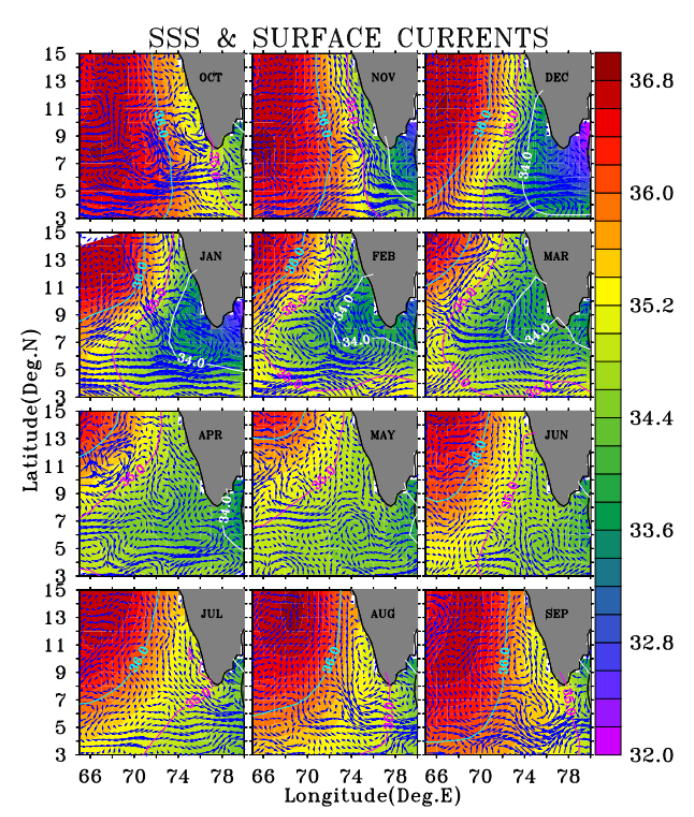


Figure 2. Surface circulation and surface salinity variation in the SEAS during 2016-17.

In winter, the southward East India Coastal current (EICC) in the southern BoB turns around Sri Lanka and flow westwards. This current strengthens from November to January. The North Equatorial Current (NEC) transport low saline waters to the southern tip of India, with one branch bifurcating northward as the West India Coastal Current (WICC). During this season, an anticyclonic eddy develops on November in the SEAS, becoming intense in January-February and dissipating by June. This eddy modifies the meridional SSS pattern, recirculating the low saline BBW in the area and spreading it southwestward due to prevailing anticyclonic circulation patterns, corroborating Ambica Behera's1 findings. In April, SSS begins to rise, and the 36, 35, and 34 psu contours gradually spread southeast, indicating the cessation of low-salinity intrusion. By June, SSS peaks at over 35.6 psu across most of the SEAS as surface currents flow predominantly equatorward, marking the onset of summer monsoon circulation. These currents carry the ASHSW, and by September, high salinity protrudes towards the Bay of Bengal<sup>5,18-21</sup>. This eddy modifies the meridional SSS pattern, recirculating the low-saline BBW in the area and spreading it southwestward due to prevailing anticyclonic circulation patterns, corroborating Behera<sup>1</sup>, et al. The influence of mesoscale eddies on salinity variability in the Arabian Sea was emphasized by Kumar and Prasad4.

Many studies have described the WICC as flowing southward in the summer monsoon, with its maximum intensity observed along the southwest coast of India<sup>22-23</sup>. The seasonal circulation patterns, particularly the SMC, WMC, WICC, and EICC, play a critical role in modulating water mass exchange between the Arabian Sea and the Bay of Bengal<sup>20-21,24-25</sup>. The

seasonal intrusion of BBW during winter and its replacement by ASHSW during summer monsoon, driven by these currents, is crucial for understanding the SEAS hydrography and its impact on acoustic propagation.

# 3.2 Intrusion of Low-Saline Bay of Bengal water

To study the intrusion and spreading of low-saline Bay of Bengal water, we analysed the salinity differences ( $\Delta s$ ) between salinity maximum (Smax) and surface salinity (S0) (Fig. 3). A salinity difference of 1 psu is considered substantial, exhibiting the presence of low-salinity intrusions in the region. By November, the presence of low-salinity water from BoB becomes evident in the southern SEAS. During this period, the salinity difference often exceeds 2 psu, with the intrusion lasting until January. This low salinity water spreads southeastward and moves towards north along the coastal region (Fig. 3). The spread becomes particularly pronounced in April, gradually diminishing in May, and completely dissipating by June due to the reversal of circulation patterns during the summer monsoon. One of the factors sustaining this lowsalinity waters in the region is attributed to the influence of anti-cyclonic eddies. Accumulation of these low saline waters substantially supports the formation of Arabian Sea Warm Pool<sup>16</sup>. It plays a critical role in modulating both the onset and intensity of Indian summer monsoon<sup>26</sup>.

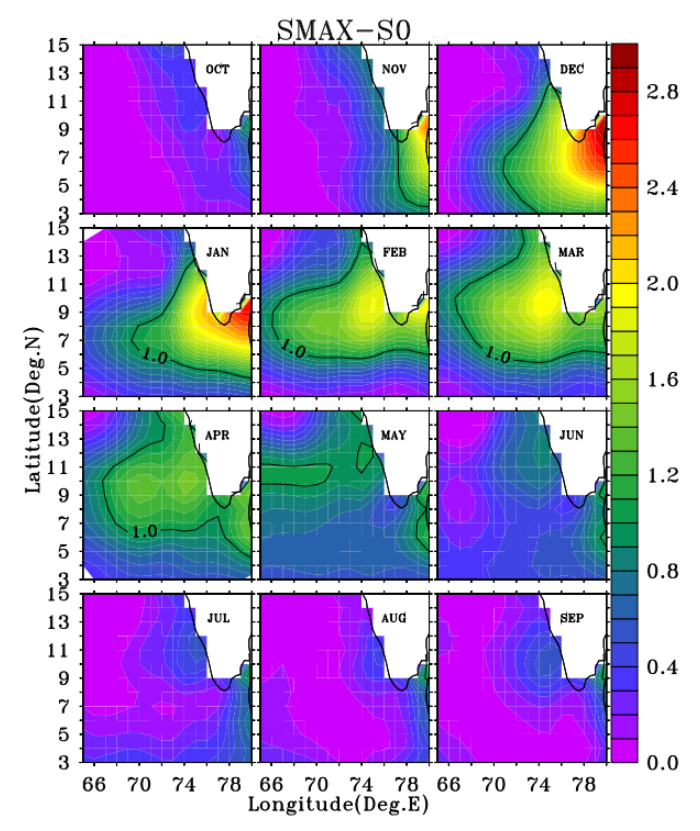


Figure 3. Monthly distribution of  $\Delta s$  (psu), difference between the Salinity maxima and Sea surface salinity in the SEAS.

# 3.3 Characteristics of ASHSW in the SEAS

To investigate the characteristics of the ASHSW in the SEAS, the core value of ASHSW and the depth of this core were plotted (Fig. 4). For this study, 35.3 psu was used as the

lower limit for ASHSW, meaning that any salinity maximum below 35.3 psu is considered as the absence of ASHSW in the region.

The analysis revealed a distinct meridional frontal pattern between eastern and western portions of SEAS. The northwestern portion exhibited less variability in salinity, while the southern tip of the SEAS showed maximum salinity variability<sup>1,27</sup>. During the summer monsoon, the ASHSW extends southward, protruding towards the southern tip of the southwest coast, with core values increasing during this season<sup>4,6</sup>.

In general, the core salinity values of ASHSW are higher during August - November, and lower during April - May. The core depth of ASHSW ranged from 20 m to 80 m, with a deepening trend towards the south. During the summer monsoon, especially from August to November, ASHSW was observed at depths of 20-40 m in most locations. During the winter monsoon, waters from the BoB intrude into SEAS further deepened the ASHSW, with core depths varying between 60 m and 80 m. Coastal currents during this period hindered the southward protrusion of ASHSW into the coastal regions, which was clearly observed during November and December. ASHSW was not evident in the southern part of the region until August, where as its maximum extent towards south was observed during September and October. This seasonal behaviour highlights the dynamic nature of ASHSW in response to monsoonal and oceanographic processes within the SEAS.

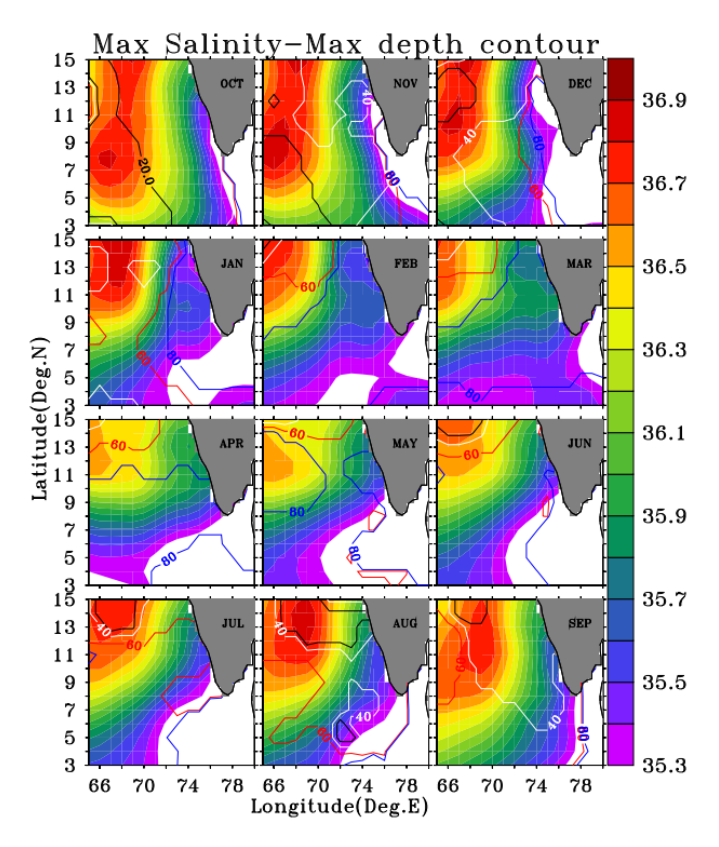


Figure 4. Monthly Distribution of salinity maxima (Smax) and Depth of Salinity maxima(Dmax) in the SEAS. Smax represented as colour contours from 35.3 psu. Dmax represented as contour lines at 20 m interval.

# 3.4 Inter-Annual Variability of BBW and ASHSW in SEAS

To examine the seasonal and inter-annual variability of BBW and ASHSW, water-mass counts were calculated as outlined in Section 2.1.3. Figure 5 clearly illustrates that BBW in the South-Eastern Arabian Sea (SEAS) exhibits strong seasonality with minimal inter-annual variability. The intrusion of BBW typically begins in November, reaches its peak by March, and fully retreats by June. ASHSW also shows a strong seasonal pattern, with its maximum (minimum) presence during the summer (winter) monsoon. It is noteworthy that both water masses experience a rapid decline in intensity. The presence of ASHSW decreases sharply from November onwards, coinciding with the development of the BBW intrusion. BBW dissipates completely in line with the onset of monsoonal circulation. In addition to this seasonal variability, ASHSW displays inter-annual variability. Specifically, ASHSW's presence was weaker during 2017 and 2020, while it was notably stronger in 2018 and 2019.

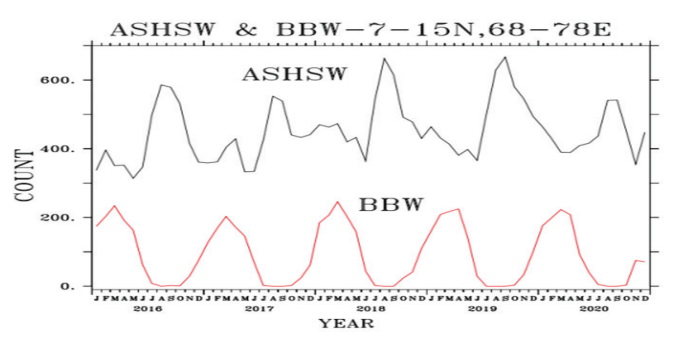


Figure 5. Inter-annual variability of BBW and ASHSW indices in the SEAS (2016-2020 in the region of 7-15  $^{\circ}$ N and 68-78  $^{\circ}$ E).

# 3.5 Role of BBW and ASHSW on Acoustic Propagation

To study the influence of BBW and ASHSW on acoustic propagation, sound speed profiles from a deep-water station located at 10 °N, 74 °E were analyzed. This station is far from the coast, minimizing the influence of coastal processes such as upwelling and down welling.

Based on the interannual variability of BBW and ASHSW in the southeastern Arabian Sea (SEAS) (Fig. 5), four representative months were selected: January and March, when BBW intrusion is at its peak, and June and October, when BBW is absent in the SEAS. The vertical profiles of temperature, salinity, and sound speed for these months are presented in the figure (Fig. 6). In general, sound speed follows the temperature profile. It is evident that during January and March, BBW dominates the surface layers, with ASHSW lying beneath it, creating a strong halocline extending from the surface to the core depth of ASHSW(66 m). In contrast, in June, BBW is absent from the surface layers, resulting in a relatively weaker halocline. During October, ASHSW occupies the upper 100 m. ASHSW is present in all four months, with its core depth ranging between 60 m and 120 m.

These findings align with previous studies highlighting the seasonal intrusion of low-salinity waters into the SEAS, modulating salinity stratification and impacting acoustic propagation<sup>28</sup>.

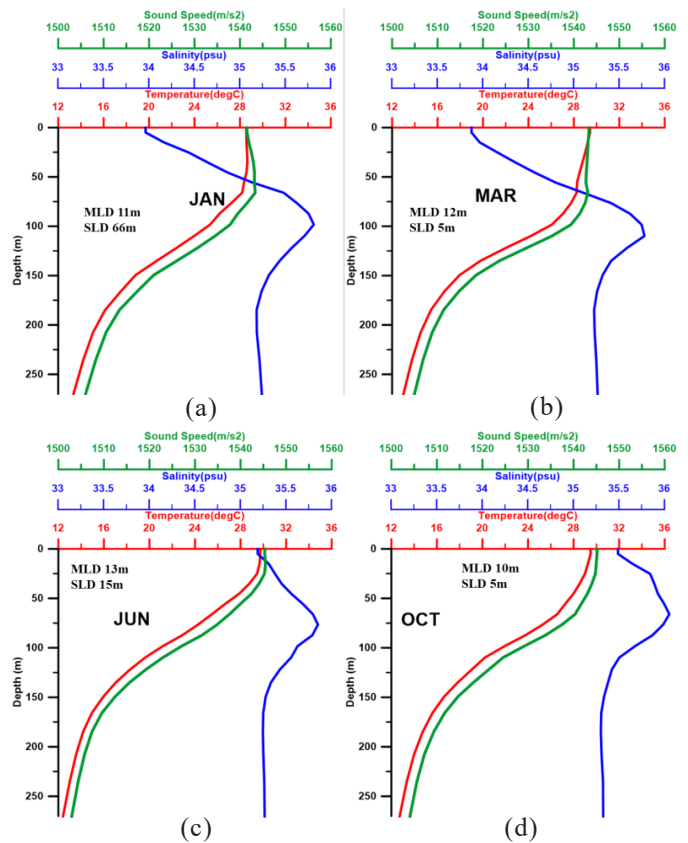


Figure 6. Vertical distribution of Temperature, Salinity & SSP at 10 °N; 74 °E for (a) Jan; (b) Mar; (c) Jun; and (d) Oct.

Mixed Layer Depth (MLD) remains shallow (10–15 m) in all four months. This is primarily due to BBW intrusion in January, while in March, weak winds and low-salinity BBW waters contribute to the shallow MLD. The shallow MLD in June is likely due to upwelling, with a strong thermocline observed below it. The shallow MLD in October is associated with weak winds and a secondary temperature maximum, a common feature in the SEAS. The Sonic Layer Depth (SLD) remains shallow in all months except January. In January, SLD reaches 66 m, likely due to a deep isothermal layer (76 m) and a strong halocline formed by the two water masses. Although the BBW forms a strong halocline in March, weak winds and strong radiative fluxes result in a shallow isothermal layer(35m), keeping the SLD shallow. However, the presence of a strong halocline leads to weak sound speed gradients below the SLD. Studies have reported similar trends, emphasizing the role of seasonal salinity stratification in modulating MLD and SLD 29-31.

The SLD determines a Minimum Cutoff Frequency (MCF), beyond which sound waves are typically confined within the surface duct. The MCF values for January, March, June, and October are 255 Hz, 16,000 Hz, 3,095 Hz, and 16,000 Hz, respectively.

To examine transmission loss (TL) characteristics, TL modeling was conducted for the four profiles using the Bellhop model at a frequency of 1,000 Hz. Four source depths were considered: 5 m (within the layer), 25 m (below the layer for all profiles except January), and 75 m (at the ASHSW core).

The TL mosaic for these profiles is presented in Fig. 7. TL values above 100 dB are marked as white spaces, while values between 40 dB and 100 dB are represented as color mosaics transitioning from red to blue.

For a source depth of 5 m, strong ducted propagation was observed in January, whereas March, June, and October did not exhibit ducted propagation, as 1,000 Hz is much lower than their respective MCFs. However, in March, relatively better TL was observed due to the weak sound speed gradient associated with BBW intrusion.

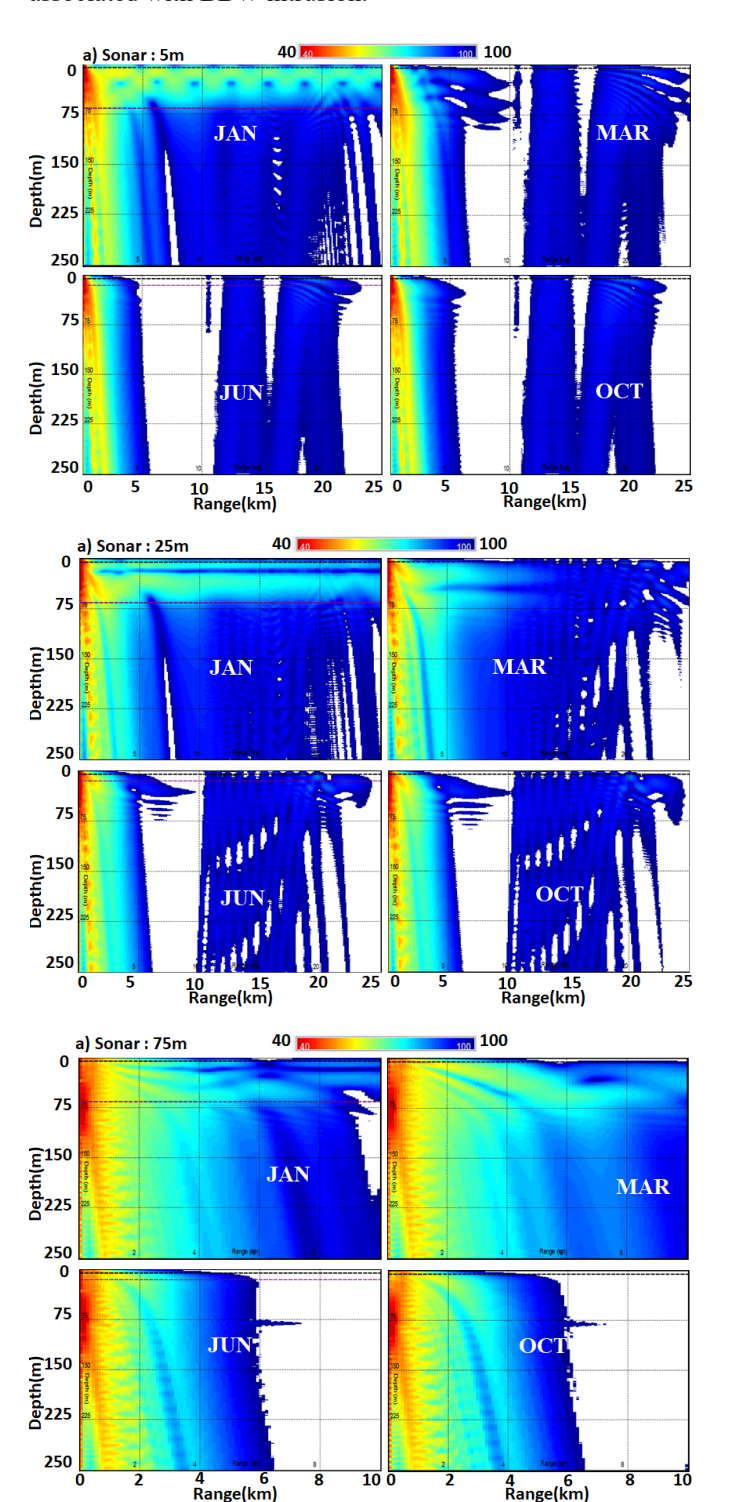


Figure 7. Depth-range plots of transmission loss.

If the source is placed at 25 m, it remains within the surface duct in January, whereas for the other months, it is positioned below the layer. Consequently, TL modeling shows poor detection for these months. However, in March, due to the weak sound speed profile (SSP) below the surface duct—caused by the presence of a strong halocline—relatively better TL mosaics are obtained. Similarly, when the sonar is positioned at 75 m, TL modeling indicates better performance in January and March compared to June and October.

To quantify the TL values, TL vs. range plots for all profiles are presented in Fig. 8. When both the source and receiver are placed at 5 m, TL values remain low in January,

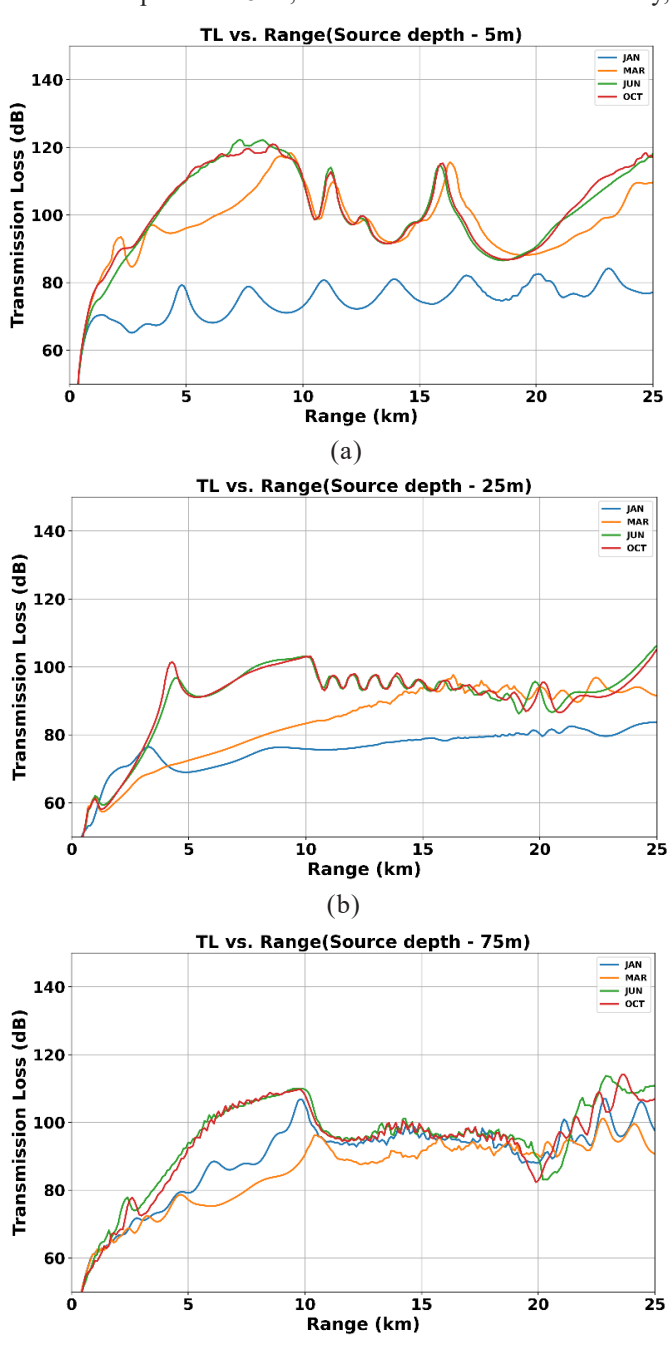


Figure 8. Range vs. Transmission Loss (TL) plots for four profiles (January, March, June, and October) with the source and receiver positioned at (a) 5 m, (b) 25 m, and (c) 75 m.

(c)

generally below 80 dB at a 25 km range. In contrast, for the other profiles, TL increases rapidly, exceeding 100 dB within just 5 km (Fig. 8(a)). For the source and receiver at 25 m depth (Fig. 8(b)), TL values remain below 80 dB up to approximately 10 km in January and March, whereas (TL) mosaics for four profiles (January, March, June, and October) with the sonar positioned at (a) 5 m, (b) 25 m, and (c) 75 m. TL modeling is performed at a frequency of 1000 Hz using the Bellhop model. The X-axis represents range (km), and the Y-axis denotes depth (m).

For June and October, TL reaches 100 dB within the same range. Similarly, for the source and receiver at 75 m depth (Fig. 8(c)), the direct path over a 10 km range shows distinct TL variations across all profiles, with TL being the lowest in March (~90 dB) and significantly higher in June and October (>120 dB). This is likely due to weaker SSP gradients in March.

These results demonstrate that seasonal changes in BBW and ASHSW play a crucial role in shaping the acoustic environment of SEAS. The interplay between salinity-driven stratification and thermal variability significantly influences sound propagation, with implications for sonar performance and underwater communication system.<sup>32</sup>

### REFERENCES

- Behera A, Vinayachandran PN, Shankar D. Influence of rainfall over eastern Arabian Sea on its salinity. J Geophys Res Oceans. 2019;124(6):5003–20.
- Fekete BM, Vorosmarty CJ, Grabs W. High-resolution fields of global runoff combining observed river discharge and simulated water balances. Global Biogeochem Cycles. 2002;16(3):15-1.
- Han W, McCreary JP. Simulation of seasonal and interannual variability in the Indian Ocean. J Phys Oceanogr. 2001;31(8):2022-2049.
- Kumar SP, Prasad TG. Formation and spreading of Arabian Sea high-salinity water mass. J Geophys Res Atmos. 1999;104(C1).
- Prasad TG, Ikeda M. The seasonal and interannual variability of sea surface salinity in the Arabian Sea. J Geophys Res Oceans. 2002;107(C9):3199.
- Thoppil PG. Mesoscale eddy modulation of winter convective mixing in the northern Arabian Sea. Deep Sea Res Part II. 2024;216:105397.
- Donguy JR, Meyers G. Seasonal variations of sea surface salinity and temperature in the tropical Indian Ocean. Deep Sea Res Part I Oceanogr Res Pap. 1996;43(2):117– 38.
- 8. Hareeshkumar PV. Seasonal variations of upper ocean temperature and salinity in the eastern Arabian Sea. Indian J Mar Sci. 1997;26(2):145–50.
- 9. Hareeshkumar PV, Mathew B. Salinity distribution in the Arabian Sea. Indian J Mar Sci. 1997;26:271–277.
- 10. Martin MV, Venkatesan R, Weller RA, et al. Seasonal temperature variability observed at abyssal depths in the Arabian Sea. Sci Rep. 2022;12:15820.
- 11. Sharma R, Kumar S, Prasad TG. Seasonal variability of salinity in the Arabian Sea. J Clim. 2010;23(16):4337–55.
- 12. Vinayachandran PN, Nanjundiah RS. Indian Ocean sea

- surface salinity variations in a coupled model. J Clim. 2009;22(13):3167–86.
- 13. Parekh A, Chowdary JS, Sayantani O, et al. Tropical Indian Ocean surface salinity bias in Climate Forecasting System coupled models and the role of upper ocean processes. Clim Dyn.2016;46:2403–22.
- 14. Jensen TG. Arabian Sea and Bay of Bengal exchange of salt and tracers in an ocean model. Geophys Res Lett. 2001;28(20):3967–70.
- 15. Thadathil P, Shankar D, Ghosh AK. Surface layer temperature inversion in the eastern Arabian Sea. Deep Sea Res Part I Oceanogr Res Pap. 2008;55(2):223–39.
- 16. Nyadjro ES, Subrahmanyam B, Murty VSN, Shriver JF. The role of salinity on the dynamics of the Arabian Sea mini warm pool. J Geophys Res Oceans. 2012;117(C9):3040.
- 17. Roman-Stork HL, Subrahmanyam B, Murty VSN. The role of salinity in the southeastern Arabian Sea in determining monsoon onset and strength. J Geophys Res Oceans. 2020;125:e2019JC015592.
- 18. Jain V, Shankar D, Vinayachandran PN, et al. Evidence for the existence of Persian Gulf Water and Red Sea Water in the Bay of Bengal. Clim Dyn. 2016;48(9–10):3207–26.
- 19. Murty VSN, Sarma YVB, Rao DP, Murty CS. Water characteristics, mixing and circulation in the Bay of Bengal during southwest monsoon. J Mar Res. 1992;50:207–28.
- 20. Shankar D, Vinayachandran PN, Unnikrishnan AS. The monsoon currents in the north Indian Ocean. Prog Oceanogr. 2002;52(1):63–120.
- 21. Vinayachandran PN, Shankar D, Vernekar S, Sandeep KK, Amol P, Neema CP, Chatterjee A. A summer monsoon pump to keep the Bay of Bengal salty. Geophys Res Lett. 2013;40:1777–82.
- 22. Shenoi SSC. Intra-seasonal variability of the coastal currents around India: A review of the evidences from new observations. Indian J Mar Sci. 2010;39(4).
- 23. Shetye SR. West India Coastal Current and Lakshadweep High/Low. Sadhana. 1998;23(5–6):637–51.
- 24. Durand F, Shankar D, Birol F, Shenoi SS. An algorithm to estimate coastal currents from satellite altimetry: A case study for the east coast of India. Remote Sens Environ. 2004;93(4):353–66.
- 25. Jensen TG, Wijesekera HW, Nyadjro ES, et al. Modeling salinity exchanges between the equatorial Indian Ocean and the Bay of Bengal. Oceanography. 2016;29(2):92101.
- 26. Neema CP, Hareeshkumar PV, Babu CA. Characteristics of Arabian Sea mini warm pool and Indian summer monsoon. Clim Dyn. 2012;38:2073–87.
- 27. Shee A, Sil S, Gangopadhyay A. Recent changes in the upper oceanic water masses over the Indian Ocean using Argo data. Sci Rep.2023;13:20252.
- Srinivasu K, Sanjana MC, Latha G, Udaya Bhaskar TVS, Rahaman H, Thirunavukkarasu A, Venkatesan R. Study on acoustic variability affected by upper ocean dynamics in southeastern Arabian Sea. Earth Space Sci. 2024;11:e2023EA003497.
- Udaya Bhaskar TVS, Swain D. Relation between sonic layer and mixed layer depth in the Arabian Sea. Indian J Geo-Mar Sci. 2016;45(10):1264–71.

- 30. Helber RW, Barron CN, Carnes MR, Zingarelli RA. Evaluating the sonic layer depth relative to the mixed layer depth. J Geophys Res. 2008;113(C7).
- 31. Maheswaran PA, Kumar SS, Kumar TP. Intra-annual Variability of the Arabian Sea High Salinity Water Mass in the South-Eastern Arabian Sea during 2016-17. Def Sci J. 2019;69(2):149–55.
- 32. Felton CS, Subrahmanyam B, Murty VSN, Shriver JF. Estimation of the barrier layer thickness in the Indian Ocean using Aquarius Salinity. J Geophys Res:Oceans. 2014;119(7):4200–4213.

#### **ACKNOWLEDGEMENT**

Authors are thankful to Dr. Duvvuri Seshagiri, Director, DRDO-NPOL, Kochi, Kerala, India, for his encouragement and motivation to carry out this study. The support provided by Dr. A Raghunadha Rao, Group Director, Ocean Science Group is greatly appreciated.

# **CONTRIBUTORS**

**Ms Anjali K.S.** obtained her MTech (Ocean Technology) from Cochin University of Science and Technology (CUSAT), Kochi, Kerala and working as Senior Research Fellow at DRDO-NPOL,

Kochi. Her research areas include: Hydrography, circulation and water mass in the North Indian Ocean and Ocean acoustics. In the current study, she did the processing, analysis, plotting and manuscript writing.

**Dr P.A. Maheswaran** obtained his PhD in Oceanography from Cochin University of Science and Technology, Kochi, Kerala and working as a Scientist at DRDO-NPOL, Kochi. His research areas include: Mixed layer dynamics, observational oceanography, sonar Oceanography.

In the present study, he formulated the concept and research objective. He guided for the study and also carried out the editing of the paper.

**Dr K. Satheesh Kumar** obtained his PhD from Cochin University of Science and Technology and working as Scientist at DRDO-NPOL, Kochi. His field of specialisation include: Underwater acoustics, sonar performance modelling, operator theory, etc. In the current study, he done the acoustic propagation modelling, manuscript editing and review.

Mr Dominic Ricky Fernandez obtained his Masters and from Cochin University of Science and Technology and working as a Scientist at DRDO-NPOL, Kochi. His field of specialisation include: Ocean data management, physical Oceanography. In the current study, he did the analysis, plotting and also carried out manuscript editing and review.